ACS NANO

www.acsnano.org

ARTICLE

Fully Screen-Printed, Large-Area, and Flexible Active-Matrix Electrochromic Displays Using Carbon Nanotube Thin-Film Transistors

Xuan Cao,[†,⊥] Christian Lau,[‡,⊥] Yihang Liu,[‡] Fanqi Wu,[†] Hui Gui,[†] Qingzhou Liu,[†] Yuqiang Ma,[‡] Haochuan Wan,[†] Moh. R. Amer,[§,∥] and Chongwu Zhou*[,†,‡]

[†]Department of Materials Science and [‡]Department of Electrical Engineering, University of Southern California, Los Angeles, California 90089, United States

[§]Department of Electrical Engineering, University of California, Los Angeles, California 90095, United States

[∥]Center of Excellence for Green Nanotechnologies, King Abdulaziz City for Science and Technology, Riyadh 12371, Saudi Arabia

Supporting Information

ABSTRACT: Semiconducting single-wall carbon nanotubes are ideal semiconductors for printed electronics due to their advantageous electrical and mechanical properties, intrinsic printability in solution, and desirable stability in air. However, fully printed, large-area, high-performance, and flexible carbon nanotube active-matrix backplanes are still difficult to realize for future displays and sensing applications. Here, we report fully screen-printed active-matrix electrochromic displays employing carbon nanotube thin-film transistors. Our fully printed backplane shows high electrical performance with mobility of 3.92 ± 1.08 $cm^2 V^{-1} s^{-1}$, on−off current ratio $I_{on}/I_{off} \sim 10^4$, and good uniformity. The printed backplane was then monolithically integrated with an array of printed electrochromic pixels, resulting in an entirely screen-printed active-matrix electrochromic display (AMECD) with good switching characteristics, facile manufacturing, and long-term stability. Overall, our fully screen-printed AMECD is promising for the mass production of large-area and low-cost flexible displays for applications such as disposable tags, medical electronics, and smart home appliances.

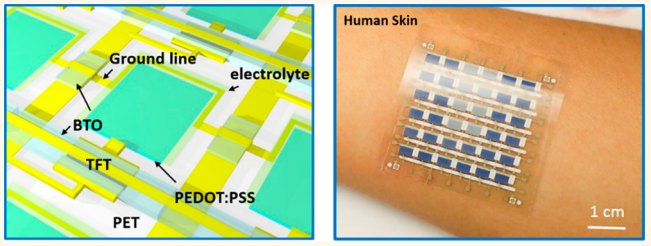

KEYWORDS: *single-wall carbon nanotubes, screen printing, thin-film transistors, active-matrix backplane, electrochromic display*

Printed electronics enable additive patterning, solution-based processing at low-temperatures, outstanding scalability, and the elimination of high-vacuum conditions.[1,2] Compared with conventional microfabrication, printing simplifies the manufacturing process from multistage photolithography and deposition to one-step additive patterning,[1] which dramatically accelerates the manufacturing process. Furthermore, the processing temperature for printing technology is typically below 130 °C,[1] which is compatible with commonly used flexible plastic substrates such as polyethylene terephthalate (PET) and polyethylene naphthalate (PEN). Printing is also a solution-based patterning technique and does not require high-vacuum conditions needed in conventional material deposition processes such as metal evaporation, atomic layer deposition, and so on. As a result, printed electronics can remarkably reduce the cost of manufacturing and thus enable large-area, low-cost, and flexible displays for various applications such as disposable tags, single-use medical electronics, and smart home appliances.[3−7]

Due to the aforementioned advantages, printed displays have attracted growing interest among the research community.[8−10] Although considerable efforts have been spent on developing printed organic light-emitting diodes (OLEDs),[11,12] progress has been hampered by the poor stability of organic molecules against moisture. Instead, researchers have recently focused their attention on developing printed polymer light-emitting diodes (PLEDs) and quantum-dot light-emitting diodes (QLEDs).[9,13−15] These devices require the ability to print thin layers to achieve a relatively low operation voltage. Meanwhile, the surface roughness should also be minimized to avoid leakage current that leads to nonradiative recombination of electrons and holes. In this regard, inkjet printing satisfies these requirements and has been used to fabricate PLEDs and QLEDs. However, the low throughput of inkjet printing is problematic for the mass production of large-area displays.[3] Electroluminescent displays (EL) are another group of light-emitting devices and can be printed using high-throughput and

Received: August 9, 2016
Accepted: October 13, 2016

DOI: 10.1021/acsnano.6b05368
ACS Nano XXXX, XXX, XXX−XXX

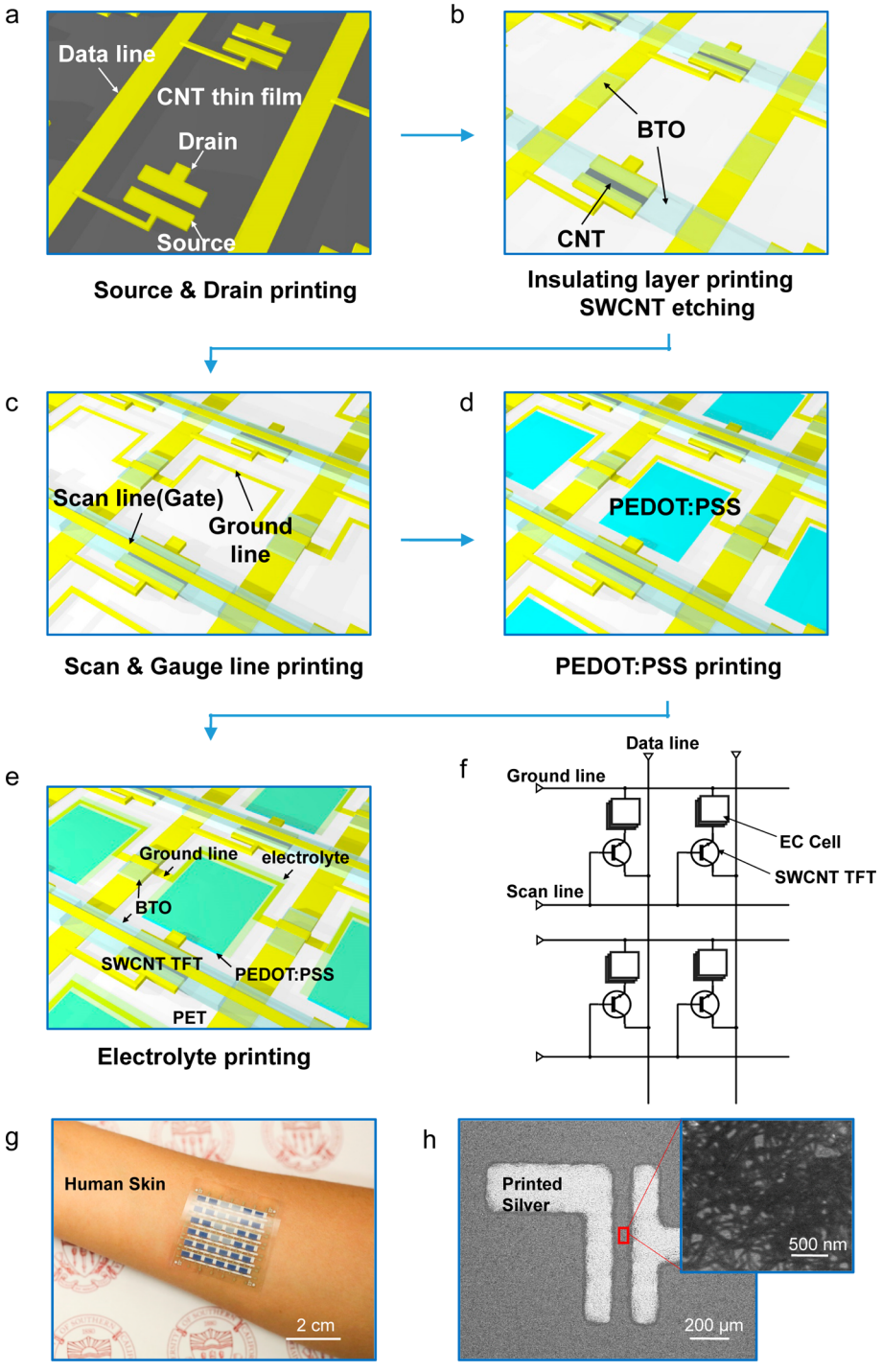

Figure 1. Fully screen-printed active-matrix electrochromic display on flexible substrate. (a–e) Schematic diagram showing the fabrication process and structure of a fully printed AMECD. (f) Circuit diagram showing the configuration of as-printed AMECD. (g) A photograph of 6 × 6 pixel flexible AMECD laminated on human skin displaying English letter "U". (h) SEM image showing the printed silver electrodes. The inset shows an SEM image of the SWCNT network in the channel region. The use of the logo in (g) has been authorized by the University of Southern California.

scalable printing techniques such as screen printing and gravure printing.[16] Nevertheless, most printed EL displays usually operate at relatively high voltage to achieve a desirable brightness (>50 V),[17,18] limiting their application due to their high-power consumption and safety concerns.

Electrochromic displays are a group of reflective displays that can reversibly change their reflectivity upon the application of a bias voltage.[8] Because electrochromic materials like poly(3,4-ethylenedioxythiophene) polystyrenesulfonate (PEDOT:PSS) fundamentally operate by reflecting light rather than emitting, electrochromic displays are more comfortable for reading and can serve as a nonvolatile display with extremely low-power consumption. Due to their device configuration, low operation voltage, and solution-based fabrication process, electrochromic displays are ideal candidates for printed displays.[19−22] Nevertheless, electrochromic displays are especially susceptible to

DOI: 10.1021/acsnano.6b05368
ACS Nano XXXX, XXX, XXX−XXX

cross-talk, in which adjacent pixels are partially activated upon addressing a single pixel. This cross-talk issue can be solved by integrating electrochromic pixels into an active-matrix structure. Scientists have thus made great strides in fabricating active-matrix electrochromic displays (AMECD).[8,22] However, in those studies, the active-matrix backplane was configured by printing organic thin-film transistors, which unfortunately showed rather low mobility (<0.01 $cm^2/(V\ s)$) .[22] Also, those studies employed multiple patterning techniques such as bar coating, inkjet printing, screen printing, and lamination to fabricate a single electrochromic device,[12] which remarkably increased the complexity of manufacturing.

Our group has focused on screen printing in consideration of its inherent scalability and the simplicity of layer alignment performed in a parallel-plate fashion.[3] Here, we report fully screen-printed active-matrix backplanes on PET substrates using silver (Ag) nanoparticles as the conductor, semiconducting single-wall carbon nanotubes (SWCNTs) as the conduction channel, and barium titanate (BTO) as the insulator. The as-printed thin-film transistors (TFTs) in the active-matrix backplane show an outstanding carrier mobility of $3.92 \pm 1.08\ cm^2\ V^{-1}\ s^{-1}$, current on−off ratio $I_{on}/I_{off} \sim 10^4$, and good uniformity, resulting in an excellent platform for active-matrix-based display and sensing systems. Additionally, we have developed fully screen-printed electrochromic cells configured using a silver/electrolyte/PEDOT:PSS lateral structure with great ambient stability and cyclability. Combining these two components, we successfully demonstrated a fully screen-printed active-matrix electrochromic display.

Compared to other work on AMECD,[8,22] we have reduced the complexity of manufacturing by only using screen printing for all the patterning processes. Therefore, the cost of printed large-area flexible AMECD is further reduced by the simplified printing process, which is important for the mass production of large-area reflective displays. Also, SWCNT TFTs are promising for flexible and printed displays due to their outstanding electronic performance, printability, and mechanical flexibility.[23−28] In this study, SWCNT TFTs configured by silver electrodes and BTO dielectric layers show more advantageous performance and stability than organic TFTs and hence play a better role in active-matrix backplanes. Finally, in previous work on AMECD,[22] PEDOT:PSS was employed as the conducting lines connecting pixels, which caused considerable voltage loss due to its poor conductivity. Instead, we have replaced PEDOT:PSS with silver lines to avoid any considerable voltage loss. However, we only used PEDOT:PSS in the electrochromic pixels as the active material showing color change by oxidation and reduction. The Ag/electrolyte/PEDOT:PSS lateral structure we developed for electrochromic cells shows good functionality, manufacturability, and stability. Overall, we believe the fully screen-printed flexible active-matrix electrochromic display using SWCNT TFTs, with outstanding electrical performance and cost-effective fabrication process, establishes a promising platform for low-cost, large-area, and flexible printed displays.

RESULTS/DISCUSSION

The fabrication process of the active-matrix electrochromic display is outlined in Figure 1a−e. First, high-purity semiconducting SWCNTs were incubated on a 5 × cm^2 PET substrate. Second, silver source and drain electrodes and data lines were printed, followed by the printing of a BTO layer on the channel region of each TFT, as shown in Figure 1a. The printed BTO layer was used as a hard mask for oxygen plasma etching to remove the unwanted SWCNTs outside the TFT region and avoid crosstalk between adjacent pixels (Figure 1b). Then another BTO layer was printed as a passivation layer to protect the data lines and the ground lines. Finally, scan lines, ground lines, PEDOT:PSS layer, and electrolyte were screen printed sequentially, as shown in Figure 1c−e. Figure 1f is a circuit diagram of the as-printed AMECD, where each pixel is composed of a SWCNT TFT and an electrochromic cell. Figure 1g is a photograph of a fully screen-printed AMECD laminated on human skin, displaying the letter "U" with excellent color contrast. The detailed procedure for operating the as-printed AMECD will be described below. Figure 1h and inset are scanning electron microscopy images showing printed Ag source/drain and SWCNT network in the channel.

A key step toward a fully screen-printed AMECD is to optimize the device performance and uniformity of the printed SWCNT TFT array. The electrical characteristics are shown in Figure 2. In this work, the printed backplane contains 6 × 6

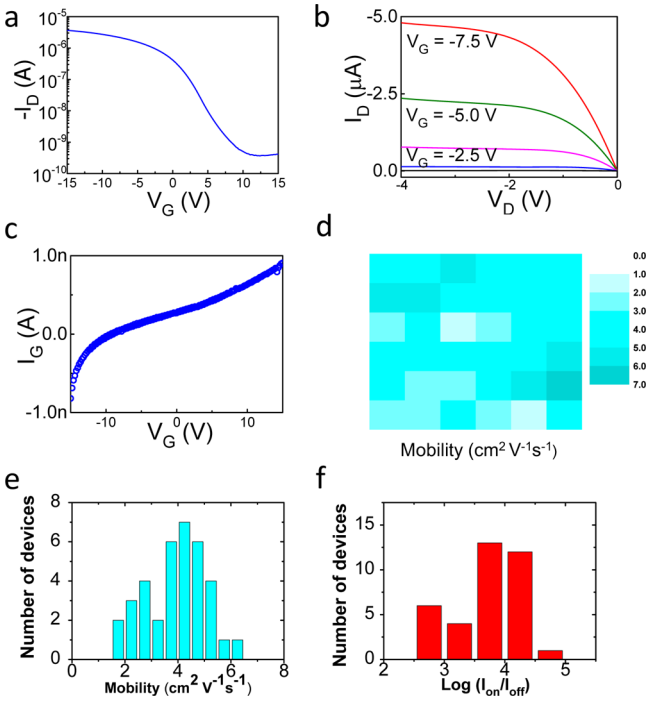

Figure 2. Electrical characterization of a fully screen-printed SWCNT backplane. (a) Transfer characteristics of a representative TFT measured at V_{DS} = −1 V. (b) Output characteristics of the same device. V_G is from −7.5 V to −2.5 V in 2.5 V steps. (c) Gate leakage current as a function of gate voltage at V_{DS} = −1 V. (d) Mobility map of an as-printed 6 × 6 active-matrix backplane. (e, f) Histograms of mobilities and current on−off ratios for 36 TFTs in the backplane, showing mobility =3.92 ± 1.08 $cm^2\ V^{-1}\ s^{-1}$ and $\log(I_{on}/I_{off})$ = 3.71 ± 0.55.

SWCNT TFTs with channel length (L) ∼ 105 μm and channel width (W) ∼ 1000 μm. Based on the recipe we reported in previous work,[3] diluted inks were used for source, drain, and dielectric layer patterning, whereas the gate was printed with undiluted silver ink, resulting in thicknesses of 3 μm for both the source and drain, 5 μm for the BTO dielectric layer, and 10 μm for the gate. Figure 2a shows the transfer characteristics of a representative SWCNT TFT at source drain voltage (V_{DS}) = −1 V, exhibiting on-state current density of 3.62 μA/mm at

DOI: 10.1021/acsnano.6b05368
ACS Nano XXXX, XXX, XXX−XXX

gate voltage (V_G) = −15 V with an average on−off ratio of 10^4. The output characteristics of the same device in the saturation region and linear region are shown in Figure 2b, suggesting the pinch-off effect and good ohmic contact between the SWCNT network and silver electrodes. Moreover, the dependence of gate leakage current on gate voltage is illustrated in Figure 2c. Overall, with applied V_{DS} = −1 V, the gate leakage current is smaller than 1 nA in the range of V_G from −15 to 15 V, indicating the high quality of as-printed BTO for the gate dielectric. In this work, we used the parallel plate model to extract the mobility of printed TFTs, as done in our previous work[3,29] and detailed in Supporting Information. Accordingly, the statistical study of the mobility of our 6 × 6 TFT array is shown by the mobility mapping in Figure 2d as well as the histogram in Figure 2e. As shown, the average mobility obtained is ∼3.92 $cm^2\ V^{-1}\ s^{-1}$ with a standard deviation ∼1.08 $cm^2\ V^{-1}\ s^{-1}$. Similarly, I_{on}/I_{off} ratio of this TFT array is shown in Figure 2f, with a $\log(I_{on}/I_{off})$ having an average of 3.71 and a standard deviation of 0.55. Based on these statistical data, the outstanding electrical performance of the fully screen-printed TFT array is comparable with Javey and Cho's work on gravure printed CNT TFTs[24] and backplanes.[30,31] This enhanced electrical performance can enable new applications such as monolithically integrated active-matrix organic light-emitting diode (AMOLED), which requires relatively high mobility. On the other hand, we believe the excellent uniformity of the as-made 6 × 6 pixel backplane is desirable for practical applications such as large-area active-matrix-based flexible displays and sensing systems.

It should be noted that considerable effort was spent on developing fully screen-printed electrochromic cells. When designing printed electrochromic cells, there are two possible configurations: a lateral configuration and a vertical configuration. The lateral structure consists of two electrodes and a layer of electrolyte bridging them.[32] In the vertical structure, the electrolyte is sandwiched between two electrodes. Compared with the lateral structure, the vertical structure effectively reduces the carrier path length to the thickness of electrolyte, resulting in a more rapid color switching response. However, for printing processes, the vertical structure may cause current leakage between the two electrodes for several reasons. First, the printed electrolyte may not be very dense or flat, and pinholes can be induced after printing the top electrode when the solvent is evaporated during baking. Because all the materials are formulated into solution-based inks to facilitate the printing process, the solvent employed to carry electrode materials such as PEDOT may also dissolve a portion of printed electrolyte, consequently creating more pinholes. Previously, a lamination technique, using electrodes patterned on two separate substrates and a layer of electrolyte in between as an adhesion layer, was employed to avoid the leakage issue.[22]

In an effort to avoid the lamination step and further simplify the manufacturing process, we have chosen the lateral structure to facilitate the screen printing process. Based on our observations, the switching time of our electrochromic cells is about 2−5 s, which is consistent with previous reports of lateral electrochromic cells.[8] The screen-printed electrochromic cell consists of three components: ground lines, electrolyte, and PEDOT:PSS as the active material for coloration. For every smart pixel, there exists one TFT integrated with an EC cell. Notably, compared with the other published work on printed electrochromic displays,[8,20−22,32] all the layers of our smart pixels were deposited using screen printing. This eliminates the needs for combining multiple patterning techniques like bar coating, inkjet printing, lamination, and so on. Furthermore, with the high throughput, scalability, and relatively accurate alignment, the screen printing method is highly desirable for mass production of large-area printed electronics. Therefore, the simplicity of our fabrication scheme with screen printing would be important for practical applications of printed backplanes due to the low cost, simple, and fast processing.

Figure 3a is a schematic diagram showing the printed lateral-structure EC cell. The thickness profiles of the printed silver

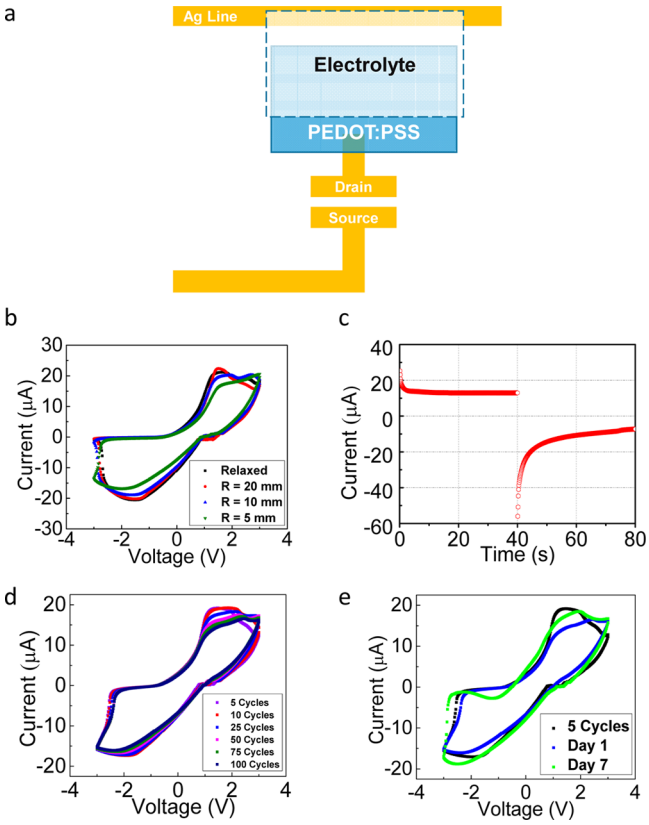

Figure 3. Electrical characteristics of fully printed flexible electrochromic cells. (a)Top view schematic diagram showing the lateral structure of a printed EC cell. (b) I−V characteristics of a printed electrochromic cell under relaxed state and bent to various radiuses. (c) Switching characteristics of a printed electrochromic cell, showing oxidation and reduction processes over time with voltage at 5 V and −5 V. (d) Cyclability and (e) ambient stability characterization of the fully screen-printed electrochromic display.

layer, electrolyte, and PEDOT:PSS are reported in Supporting Information, showing thicknesses of 9, 8, and 2.5 μm, respectively. The current−voltage characteristics of a printed electrochromic cell under a relaxed state and bent to radiuses of 20, 10, and 5 mm are shown in Figure 3b, which demonstrates that the printed EC cell operates reliably under bending. When the applied bias changed from −3 to 3 V, the maximum current flowing through the pixel was around 25 μA. The switching characteristics of the EC cell at 5 V and −5 V are shown in Figure 3c. The PEDOT:PSS was oxidized upon the application of ∼5 V, showing a exponentially decreasing current from 25 μA to 13 μA. On the other hand, when the voltage changed to −5 V after oxidation, a high initial current of −58 μA was observed, which was consistent with the high initial reduction current due to the electrochemical reactions occurring in the

DOI: 10.1021/acsnano.6b05368
ACS Nano XXXX, XXX, XXX−XXX

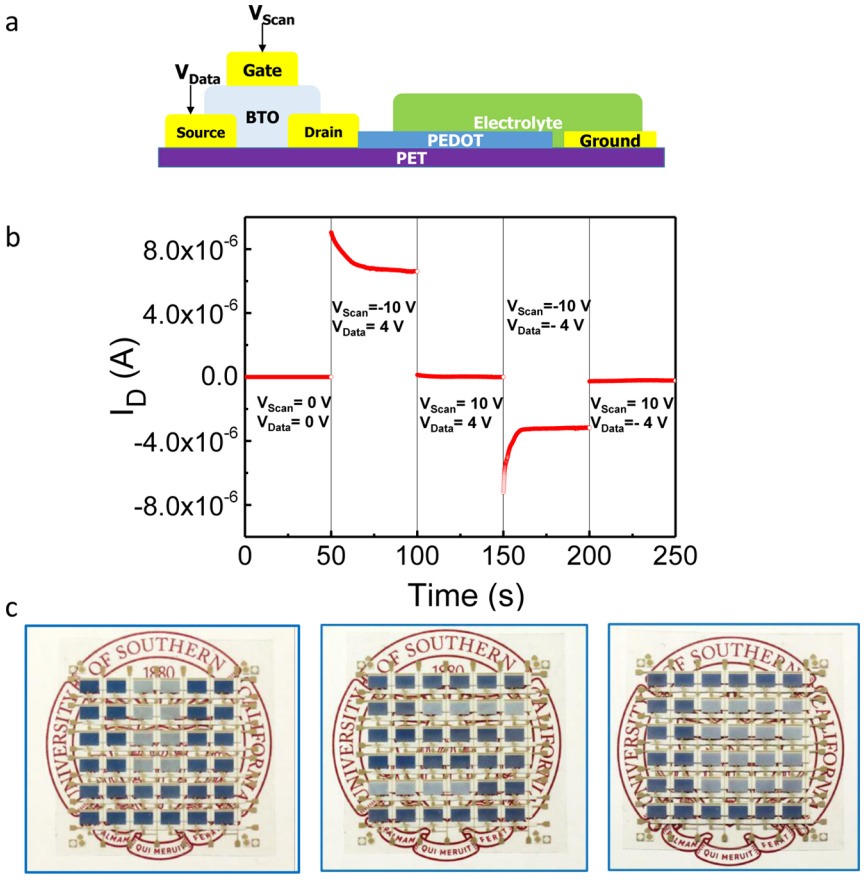

Figure 4. Fully screen-printed flexible AMECD. (a) Cross-section schematic diagram of a smart pixel in AMECD. (b) Functionality test of a smart pixel configured by a TFT and an electrochromic cell, suggesting the control capability of the TFT in turning the pixel on and off. (c) Optical images of AMECD showing letters "U", "S", and "C". The use of the logo in (c) has been authorized by the University of Southern California.

electrochromic cell.[22] However, it showed lower saturation current of −7 μA when PEDOT:PSS was reduced to a semiconducting state with lower conductivity. Figure 3d shows the similar switching characteristics of the screen-printed EC cell after sweeping bias from −3 to 3 V and then back to −3 V, for 5, 10, 25, 50, 75, and 100 cycles, suggesting excellent cyclability of the as-printed EC cell. We also carried out stability test of printed EC cells in ambient environment, as shown in Figure 3e. Negligible degradation of the electrical performance was observed after 7 days in air. The I–V characteristic measurements in Figure 3b, d, e used a sweeping rate of 20 mV between data points at 60 ms intervals. The oxidation and reduction curves in Figure 3c were taken at 100 ms intervals. Overall, we have realized fully screen-printed, lateral-structure electrochromic cells on flexible substrates with outstanding electrical performance, remarkable cyclability, and stability in ambient environment.

We have additionally realized the integration of fully printed EC cells with the printed backplane on PET substrates. Figure 4a shows the structure of a fully screen-printed smart pixel consisting of a TFT and an EC cell. Based on the measurements in Figure 3, we have carried out a functionality test of a smart pixel, as shown in Figure 4b, to demonstrate the printed TFT's control capability over the EC cell. We first built a baseline with scan line voltage (V_{Scan}) = 0 V and data line voltage (V_{Data}) = 0 V, and drain current (I_D) is ∼0 A. When V_{Scan} changed to −10 V, the TFT was switched to the on-state. With V_{Data} = 4 V, we observed a typical exponentially decreasing drain current, indicating the oxidation of PEDOT:PSS and resulting in a gray/transparent state. Then we turned the TFT off by changing V_{Scan} to 10 V, which caused the drain current to drop to 10 nA, suggesting the smart pixel remains turned off after switching off the TFT. After that, we changed the biases to V_{Scan} = −10 V and V_{Data} = −4 V. As expected, we observed the typical switching characteristics of reduction of the EC cell, showing a dark-blue PEDOT:PSS pattern. Finally, we turned the pixel off by applying V_{Scan} = 10 V. Up until this point, we have demonstrated the control capability of the screen-printed SWCNT TFT on screen-printed EC cell, showing excellent coloration and retention behavior by changing V_{Scan} and V_{Data}. Based on this result, we further addressed the pixels individually and have successfully enabled the printed AMECD to display letters "U", "S", and "C" in Figure 4c. Notably, the decoloration of the as-printed reflective EC cells is negligible after addressing, suggesting an intrinsic "memory effect" in which the pixel color is retained after the applied voltage is removed. This leads to extremely low power consumption of the reflective AMECD, as static images can be displayed for hours without having to maintain an applied voltage. This feature of electrochromic displays will be essential for practical applications in large-area, cost-effective, and flexible display electronics. Encouraged by the data above, we believe this demonstration of fully screen-printed AMECD using a SWCNT backplane establishes the foundation for future research and practical application of printed large-area, low-cost, and flexible displays.

DOI: 10.1021/acsnano.6b05368
ACS Nano XXXX, XXX, XXX−XXX

CONCLUSIONS

We have fabricated fully screen-printed active-matrix electrochromic displays based on carbon nanotube thin-film transistors on flexible substrates. In this study, 6 × 6 pixel active-matrix backplanes were fully screen printed using semiconducting-enriched SWCNTs as the channel material, leading to excellent electrical performance with mobility of 3.92 ± 1.08 cm^2 V^{-1} s^{-1} and on−off current ratios ~10^4. Then we developed fully screen-printed lateral-structured electrochromic cells, which were monolithically integrated with the printed nanotube backplane. Switching characteristics, stability, and flexibility of as-printed EC cells were investigated, suggesting excellent robustness and electrical performance of screen-printed AMECD. Our work has demonstrated that the fully screen-printed SWCNT active-matrix electrochromic display can be a desirable platform for large-area, low-cost, and flexible displays.

METHODS/EXPERIMENTAL

Separated Nanotube Deposition. Flexible, transparent PET substrates (TEKRA) were first cleaned with oxygen plasma under 100 W for 90 s. A SWCNT network was then deposited by immersing the substrate in purified semiconductor-enriched CNT solution (IsoSol-S100, Nanointegris, Inc.) for 5 min. After rising with toluene and drying with a nitrogen gun, the samples were baked in a drying oven at 125 °C for 1h.

TFT Printing. In this work, diluted solutions of silver ink (AG-959, Conductive Compounds, Inc.) and BTO ink (BT-101, Conductive Compounds, Inc.) were diluted by diethylene glycol ethyl ether acetate (Solvent 20, Conductive Compounds, Inc.). All layers were printed using a desktop screen printer (DP-320, Itochu), and the thicknesses of printed layers were measured using a profilometer (Dectak II, Veeco). The source and drain electrodes were printed on transparent PET (TEKRA) using a single layer of diluted silver ink at a clearance of 2 mm. The dielectric layer and insulating layers between overlapping silver lines were subsequently printed at the same clearance using the diluted BTO ink and undiluted BTO ink, respectively. The gate and ground lines were then printed at the same clearance using undiluted silver ink. The sample was baked at 125 °C for 10 min between each layer of printing.

Electrochromic Cell Printing. A single layer of the PEDOT:PSS paste (Orgacon EL-P-5015, AGFA) was screen printed over the exposed silver drain electrode at a clearance of 2.75 mm. The sample was then baked in an oven at 60 °C for 10 min. The electrolyte ink was composed of an aqueous poly(diallyldimethylammonium chloride) solution with molecular weight <100,000 (Sigma-Aldrich), TiO_2 powder (Kronos 2300), and poly(ethylene glycol-*ran*-propylene glycol) with number-average molecular weight ~12,000 (Sigma-Aldrich) in a 5:4:1 weight ratio. The mixture was then bath-sonicated for 20 min and then probe sonicated for 25 min. First, a double layer of the electrolyte was printed on top of the PEDOT and silver ground lines using the same clearance as the PEDOT:PSS layer and baked at 60 °C for 10 min. To improve pixel contrast and heal cracks, a third layer of the electrolyte could be printed at the same conditions and then baked again at 60 °C for 10 min. Electrical measurements were carried out using an Agilent 4156B under ambient conditions.

ASSOCIATED CONTENT

Supporting Information

The Supporting Information is available free of charge on the ACS Publications website at DOI: 10.1021/acsnano.6b05368.

(PDF)

AUTHOR INFORMATION

Corresponding Author

*E-mail: chongwuz@usc.edu.

Author Contributions

⊥These authors contributed equally.

Notes

The authors declare no competing financial interest.

ACKNOWLEDGMENTS

We would like to acknowledge the collaboration of this research with King Abdul-Aziz City for Science and Technology (KACST) via The Center of Excellence for Nanotechnologies (CEGN).

REFERENCES

(1) Aleeva, Y.; Pignataro, B. Recent Advances in Upscalable Wet Methods and Ink Formulations for Printed Electronics. *J. Mater. Chem. C* **2014**, *2*, 6436−6453.

(2) Park, S.; Vosguerichian, M.; Bao, Z. A Review of Fabrication and Applications of Carbon Nanotube Film-Based Flexible Electronics. *Nanoscale* **2013**, *5*, 1727−52.

(3) Cao, X.; Chen, H. T.; Gu, X. F.; Liu, B. L.; Wang, W. L.; Cao, Y.; Wu, F. Q.; Zhu, C. W. Screen Printing as a Scalable and Low-Cost Approach for Rigid and Flexible Thin-Film Transistors Using Separated Carbon Nanotubes. *ACS Nano* **2014**, *8*, 12769−12776.

(4) Chen, P. C.; Fu, Y.; Aminirad, R.; Wang, C.; Zhang, J. L.; Wang, K.; Galatsis, K.; Zhou, C. W. Fully Printed Separated Carbon Nanotube Thin Film Transistor Circuits and Its Application in Organic Light Emitting Diode Control. *Nano Lett.* **2011**, *11*, 5301−5308.

(5) Lilja, K. E.; Backlund, T. G.; Lupo, D.; Virtanen, J.; Hamalainen, E.; Joutsenoja, T. Printed Organic Diode Backplane for Matrix Addressing an Electrophoretic Display. *Thin Solid Films* **2010**, *518*, 4385−4389.

(6) Ryu, G. S.; Kim, J. S.; Jeong, S. H.; Song, C. K. A Printed Otft-Backplane for Amoled Display. *Org. Electron.* **2013**, *14*, 1218−1224.

(7) Xu, W.; Zhao, J.; Qian, L.; Han, X.; Wu, L.; Wu, W.; Song, M.; Zhou, L.; Su, W.; Wang, C.; Nie, S.; Cui, Z. Sorting of Large-Diameter Semiconducting Carbon Nanotube and Printed Flexible Driving Circuit for Organic Light Emitting Diode (Oled). *Nanoscale* **2014**, *6*, 1589−95.

(8) Andersson, P.; Forchheimer, R.; Tehrani, P.; Berggren, M. Printable All-Organic Electrochromic Active-Matrix Displays. *Adv. Funct. Mater.* **2007**, *17*, 3074−3082.

(9) Kim, B. H.; Onses, M. S.; Lim, J. B.; Nam, S.; Oh, N.; Kim, H.; Yu, K. J.; Lee, J. W.; Kim, J. H.; Kang, S. K.; Lee, C. H.; Lee, J.; Shin, J. H.; Kim, N. H.; Leal, C.; Shim, M.; Rogers, J. A. High-Resolution Patterns of Quantum Dots Formed by Electrohydrodynamic Jet Printing for Light-Emitting Diodes. *Nano Lett.* **2015**, *15*, 969−73.

(10) Ren, M. S.; Gorter, H.; Michels, J.; Andriessen, R. Ink Jet Technology for Large Area Organic Light-Emitting Diode and Organic Photovoltaic Applications. *J. Imaging Sci. Technol.* **2011**, *55*, 40301.

(11) Kopola, P.; Tuomikoski, M.; Suhonen, R.; Maaninen, A. Gravure Printed Organic Light Emitting Diodes for Lighting Applications. *Thin Solid Films* **2009**, *517*, 5757−5762.

(12) Tekoglu, S.; Hernandez-Sosa, G.; Kluge, E.; Lemmer, U.; Mechau, N. Gravure Printed Flexible Small-Molecule Organic Light Emitting Diodes. *Org. Electron.* **2013**, *14*, 3493−3499.

(13) Kong, Y. L.; Tamargo, I. A.; Kim, H.; Johnson, B. N.; Gupta, M. K.; Koh, T. W.; Chin, H. A.; Steingart, D. A.; Rand, B. P.; McAlpine, M. C. 3d Printed Quantum Dot Light-Emitting Diodes. *Nano Lett.* **2014**, *14*, 7017−7023.

(14) Tait, J. G.; Witkowska, E.; Hirade, M.; Ke, T. H.; Malinowski, P. E.; Steudel, S.; Adachi, C.; Heremans, P. Uniform Aerosol Jet Printed Polymer Lines with 30 Mu M Width for 140 Ppi Resolution Rgb Organic Light Emitting Diodes. *Org. Electron.* **2015**, *22*, 40−43.

DOI: 10.1021/acsnano.6b05368
ACS Nano XXXX, XXX, XXX−XXX

(15) Youn, H.; Park, H. J.; Guo, L. J. Printed Nanostructures for Organic Photovoltaic Cells and Solution-Processed Polymer Light-Emitting Diodes. *Energy Technol.* **2015**, *3*, 340−350.
(16) Lee, D. H.; Choi, J. S.; Chae, H.; Chung, C. H.; Cho, S. M. Screen-Printed White Oled Based on Polystyrene as a Host Polymer. *Curr. Appl. Phys.* **2009**, *9*, 161−164.
(17) Johnston, D.; Barnardo, C.; Fryer, C. Passive Multiplexing of Printed Electroluminescent Displays. *J. Soc. Inf. Disp.* **2005**, *13*, 487−491.
(18) Kim, J.-Y.; Bae, M. J.; Park, S. H.; Jeong, T.; Song, S.; Lee, J.; Han, I.; Yoo, J. B.; Jung, D.; Yu, S. Electroluminescence Enhancement of the Phosphor Dispersed in a Polymer Matrix Using the Tandem Structure. *Org. Electron.* **2011**, *12*, 529−533.
(19) Said, E.; Andersson, P.; Engquist, I.; Crispin, X.; Berggren, M. Electrochromic Display Cells Driven by an Electrolyte-Gated Organic Field-Effect Transistor. *Org. Electron.* **2009**, *10*, 1195−1199.
(20) Kawahara, J.; Ersman, P. A.; Engquist, I.; Berggren, M. Improving the Color Switch Contrast in Pedot:Pss-Based Electrochromic Displays. *Org. Electron.* **2012**, *13*, 469−474.
(21) Andersson Ersman, P.; Kawahara, J.; Berggren, M. Printed Passive Matrix Addressed Electrochromic Displays. *Org. Electron.* **2013**, *14*, 3371−3378.
(22) Kawahara, J.; Andersson Ersman, P.; Nilsson, D.; Katoh, K.; Nakata, Y.; Sandberg, M.; Nilsson, M.; Gustafsson, G.; Berggren, M. Flexible Active Matrix Addressed Displays Manufactured by Printing and Coating Techniques. *J. Polym. Sci., Part B: Polym. Phys.* **2013**, *51*, 265−271.
(23) Ha, M. J.; Seo, J. W. T.; Prabhumirashi, P. L.; Zhang, W.; Geier, M. L.; Renn, M. J.; Kim, C. H.; Hersam, M. C.; Frisbie, C. D. Aerosol Jet Printed, Low Voltage, Electrolyte Gated Carbon Nanotube Ring Oscillators with Sub-5 Mu S Stage Delays. *Nano Lett.* **2013**, *13*, 954−960.
(24) Lau, P. H.; Takei, K.; Wang, C.; Ju, Y.; Kim, J.; Yu, Z.; Takahashi, T.; Cho, G.; Javey, A. Fully Printed, High Performance Carbon Nanotube Thin-Film Transistors on Flexible Substrates. *Nano Lett.* **2013**, *13*, 3864−9.
(25) Xu, W.; Liu, Z.; Zhao, J.; Xu, W.; Gu, W.; Zhang, X.; Qian, L.; Cui, Z. Flexible Logic Circuits Based on Top-Gate Thin Film Transistors with Printed Semiconductor Carbon Nanotubes and Top Electrodes. *Nanoscale* **2014**, *6*, 14891−7.
(26) Cai, L.; Wang, C. Carbon Nanotube Flexible and Stretchable Electronics. *Nanoscale Res. Lett.* **2015**, *10*, 1013.
(27) Cai, L.; Zhang, S.; Miao, J.; Yu, Z.; Wang, C. Fully Printed Foldable Integrated Logic Gates with Tunable Performance Using Semiconducting Carbon Nanotubes. *Adv. Funct. Mater.* **2015**, *25*, 5698−5705.
(28) Cao, Q.; Kim, H. S.; Pimparkar, N.; Kulkarni, J. P.; Wang, C. J.; Shim, M.; Roy, K.; Alam, M. A.; Rogers, J. A. Medium-Scale Carbon Nanotube Thin-Film Integrated Circuits on Flexible Plastic Substrates. *Nature* **2008**, *454*, 495−U4.
(29) Cao, X.; Cao, Y.; Zhou, C. W. Imperceptible and Ultraflexible P-Type Transistors and Macroelectronics Based on Carbon Nanotubes. *ACS Nano* **2016**, *10*, 199−206.
(30) Lee, W.; Koo, H.; Sun, J.; Noh, J.; Kwon, K. S.; Yeom, C.; Choi, Y.; Chen, K.; Javey, A.; Cho, G. A Fully Roll-to-Roll Gravure-Printed Carbon Nanotube-Based Active Matrix for Multi-Touch Sensors. *Sci. Rep.* **2015**, *5*, 17707.
(31) Yeom, C.; Chen, K.; Kiriya, D.; Yu, Z.; Cho, G.; Javey, A. Large-Area Compliant Tactile Sensors Using Printed Carbon Nanotube Active-Matrix Backplanes. *Adv. Mater.* **2015**, *27*, 1561.
(32) Andersson, P.; Nilsson, D.; Svensson, P. O.; Chen, M. X.; Malmstrom, A.; Remonen, T.; Kugler, T.; Berggren, M. Active Matrix Displays Based on All-Organic Electrochemical Smart Pixels Printed on Paper. *Adv. Mater.* **2002**, *14*, 1460.

DOI: 10.1021/acsnano.6b05368
ACS Nano XXXX, XXX, XXX−XXX